ISSN 1066-3622. Radiochemistry, 2006, Vol. 48, No. 3, pp. 307–314. © Pleiades Publishing, Inc., 2006.
Original Russian Text © R.V. Bogdanov, A.G. Krivitskii, Yu.S. Polekhovskii, N.V. Vinogradova, 2006, published in Radiokhimiya, 2006, Vol. 48, No. 3, pp. 278–284.

Radioactivity of Vanadium Ore: Radioecological Aspects

R. V. Bogdanov[a], A. G. Krivitskii[a], Yu. S. Polekhovskii[b], and N. V. Vinogradova[c]

[a] *Chair of Radiochemistry, St. Petersburg State University, St. Petersburg, Russia*
[b] *Chair of Mineral Deposits, St. Petersburg State University, St. Petersburg, Russia*
[c] *Institute of Water Problems of the North, Karelian Scientific Center, Russian Academy of Sciences, Petrozavodsk, Karelia, Russia*

Received January 24, 2006

Abstract—Chemical and mineral composition of uranium-containing ores from the Srednyaya Padma field (Karelia) was studied to forecast radioecological consequences of commercial production of vanadium at mining of fields with uranium mineralization. Along with carnotite, tyuyamunite, and pitchblendes of several generations, this mineralization contains such secondary minerals of U(VI) as vanuranylite, sayrite, soddyite, kasolite, and vandendriesscheite. At interaction with atmospheric precipitates and ground waters in the course of industrial development of the field, this group of minerals can act as an intensive source of radioactive pollution of the regional water ecosystem.

PACS numbers: 33.60.Fy, 61.10.Nz, 89.60.Ec
DOI: 10.1134/S1066362206030180

Vanadium is widely used in industry, in particular, in metallurgy. Therefore, prospecting and development of new vanadium fields is of particular scientific and industrial interests. It is well known that vanadium ores in sediment strata (especially, in high-carbon sediments) are often accompanied by increased concentration of uranium minerals of various nature. Commercial development of such fields is often environmentally hazardous, because it can cause pollution of natural waters with uranium and products of its radioactive decay. Thus, preliminarily studies aimed to evaluate the expected risks of radioactive pollution of the environment are rather urgent. In this study we took as an example a proved but not exploited field of uranium–vanadium ores in the North-West region of the Russian Federation (Srednyaya Padma, Karelia). We performed a comprehensive study of vanadium ores including analysis of chemical and mineralogical state of uranium and leaching of uranium and some radioactive daughter elements from uranium-containing vanadium ores using model atmospheric precipitates and ground waters simulating drainage water of the Srednyaya Padma field.

EXPERIMENTAL

The petrographic and mineralogical studies were carried out using optical and electron microscopy, microprobe technique, and other analytical procedures. Transparent sections and polished sections were prepared. The petrographic study of the sections was performed on an MP-6 polarization microscope at various magnifications; the polished sections were studied in the incident light on a POLAM-P312 microscope. The photomicrographs were recorded on an NEOPHOT-21 microscope using a Videotest Morfo-3 program.

The electron microscopic studies were carried out on a CamScan IV scanning microscope equipped with a Link Isis system (Oxford Instruments), a Pentafet Super ATW energy-dispersive spectrometer, and an ABT-55 Akashi device with a Link 10/86 analyzer. The preparations were sputtered with carbon and studied simultaneously in the modes of secondary and reflected electrons at an accelerating voltage of 20–25 kV. The X-ray diffraction analysis was performed on a Geigerflex D/max-RC (Rigaku, Japan) diffractometer (CuK_α radiation).

The chemical state of uranium in minerals was studied by the method of chemical shifts of the energy of the X-ray emission bands of uranium, developed at the Chair of Radiochemistry (St. Petersburg State University). The chemical shifts were recorded on a two-meter single-crystal spectrometer designed by O.I. Sumbaev with Cochois focusing [1]; a quartz single crystal was used as a monochromator. Adjustment to the desired energy band was performed with a theodolite by calculation of the required angle from the Bragg equation. The fluorescence spectra of the

Table 1. Composition of the natural mineral water (hole no. 2852) and model solution

Ion, mg l^{-1}	Natural water	Model solution
$[NH_4]^+$	1.2	1.2
Na^+	301.5	243.1
K^+	6.7	6.7
Ca^{2+}	38.2	38.2
Mg^{2+}	33.7	0.1
Fe^{2+}	0.1	0.1
Fe^{3+}	0.4	0.4
Sum of cations	381.8	323.3
$[HCO_3]^-$	350.2	350.2
Cl^-	335.7	335.7
$[SO_4]^{2-}$	31.1	31.1
$[NO_3]^-$	0.4	0.4
Sum of anions	717.4	717.4
pH	7.81	7.81

sample excited by bremsstrahlung and characteristic radiation of the silver anode of an X-ray tube was recorded with a scintillation detector based on a NaI(Tl) crystal.

The effect of liquid phase on the uranium–vanadium ores was studied with two types of solutions: (1) model atmospheric precipitates simulated by distilled water through which air was bubbled for 24 h, causing an increase in pH from 6.9 to 7.4, and (2) model solution of ground water whose cationic and anionic composition was similar to the chloride–carbonate water from hole no. 2852 (Srednyaya Padma field). The pH of the natural water and model solution was 7.81. The chemical compositions of these waters are given in Table 1.

Before leaching, two ore samples (whose description is given below) were ground and fractionated using a set of analytical sieves into 0.50 – 0.25, 0.25–0.12, 0.12– 0.07, and <0.07-mm fractions. The sample surface area was calculated by the known procedure [2]. Several liters of the model solutions were passed through a bed of ground ore (including all the four size fraction) at a rate of 1 l in 1–3 s. Then, 100-ml aliquots were taken for α-ray spectrometry from each liter of the solution that passed through the ore bed, and the remaining solutions were used for measuring activity of β- and γ-emitters such as ^{226}Ra and the products of its decay including ^{210}Pb and ^{210}Bi.

The sources of $^{226}Ra(^{210}Pb)$ were prepared by coprecipitation with $BaSO_4$ [3], and uranium was concentrated by anion-exchange chromatography in 6 M HCl with ascorbic acid reducing agent [4]. The α-ray sources were prepared by molecular electroplating from the solution of ammonium formate and $HClO_4$ and the resulting α-ray spectra were analyzed using known programs [5].

The total β-ray activity was measured with a gas discharge detector. The γ-ray spectrometric analysis of the radionuclide composition of the samples was performed on a γ-ray spectrometer equipped with a Ge(Li) detector. No daughter isotopes of ^{232}Th in the samples were recorded in the spectra, which exhibited only γ-ray lines corresponding to the U–Ra series. In the open geochemical systems, the absolute radioactive equilibrium between radium and products of its radioactive decay can be disturbed because of the loss of radon, as was confirmed by our experimental results. The concentration of ^{238}U was calculated from the activity of radium, taking into account that the relative contributions of ^{226}Ra and ^{235}U to the spectral line at 185 keV are 0.56 and 0.44, respectively, and the concentration of ^{238}U (C_U) was calculated from the following equation:

$$C_U = (N_{185} \times 0.44 \times 68.94)/3486.5 \text{ (mg g}^{-1}\text{)},$$

where N_{185} is the total counting rate of ^{226}Ra and ^{235}U at the spectral line at 185 keV, counts h^{-1}; 68.94 mg, content of ^{238}U in the reference; 3486.5 counts h^{-1}, counting rate of uranium in the experimental measurement system. The activities of ^{226}Ra and the products of its radioactive decay were calculated taking into account the registration efficiency and intensity of the corresponding line in the γ-ray spectrum. The α-activity of the sources was recorded on a spectrometer equipped with a surface-barrier Si(Au) detector (surface area 10 cm^2, intrinsic resolution 55 keV) and an AI-1024-95-17 4096-channel analyzer; ^{232}U was used as a tracer. The absolute activity was calculated using OSGI and OSAI reference sources. The final results were normalized with respect to 1 l of the liquid phase, 1 m^2 of the sample surface area, and 1 day of the sample leaching.

RESULTS AND DISCUSSION

Petrographic and Mineralogical Analysis

In the course of petrographic and mineralogical analysis of the Srednyaya Padma field, we separated four main types of ores which can be recovered in the course of commercial mining at this field. The first type, containing almost no uranium and products of its decay, is a high-grade vanadium ore consisting of roscoelite micaite, vanadium hematite, vanadium zincochromite, and vanadium oxides and hydroxides.

Table 2. Chemical shifts δ and relative line broadening Γ of the emission X-ray lines of U, MeV

Line	Parameter	PD-3	PD-4	PD-5	PD-6
L_{α_1}	δ	-47 ± 4	-63 ± 4	-146 ± 3 (–160)	-129 ± 3 (–98)
L_{α_2}	δ	$+21 \pm 8$	$+21 \pm 8$	$+79 \pm 5$ (+89)	$+84 \pm 5$ (+79)
L_{β_1}	δ	-10 ± 5	-29 ± 4	$+81 \pm 5$ (+99)	$+86 \pm 6$ (+63)
L_{β_1}	Γ	-43 ± 40	-13 ± 22	–	–
L_{γ_6}	δ	$+219 \pm 9$	$+240 \pm 9$	$+541 \pm 12$ (+591)	$+497 \pm 11$ (+403)
L_{γ_6}	Γ	-539 ± 46	-821 ± 47	-1526 ± 71 (–1644)	-1534 ± 77 (–1422)

The content of vanadium reaches 17–18%. The radiation level of the samples of this type measured with a lead shield did not exceed normal radiation level of 10 μR h^{-1}. As seen from XRD data, the content of various vanadium-containing minerals in the ore reaches 90–95%, and roscoelite with a grain size of 0.01–0.1 mm is the main component. The content of quartz and feldspar is 5–8%, and the content of carbonate minerals (dolomite, calcite) does not exceed 1–2%. This type of ores composed the inner parts of the ore body, which occupies about 50% of the field volume.

The second type involves the lode uranium ores containing predominantly uranium oxides. At least two generations of uranium oxides were revealed: primary (uraninite) and secondary (pitchblende). This secondary phase is developed both on the periphery of the primary generation and in the inner part along the defects.

The radioactivity of the samples corresponds to the exposure dose of γ-ray radiation of 2000–3000 μR h^{-1} and over. These ores are characterized by selenide mineralization, in particular, in the form of clausthalite (PbSe). As seen from Fig. 1, clausthalite crystallizes between aggregate crystals of uraninite filling the finest pores in the mineral. The XRD data showed that this type of ores contains uraninite, pitchblende, roscoelite, clausthalite, calcite, galena, and quartz. The content of V_2O_5 in these ores varies from 2 to 10%, and their content in the ore body is about 12%. The lode ores are the most complex and contain noble metals: Pd (345–440 g t^{-1}), Pt (up to 30 g t^{-1}), Au, and Ag. One of the authors of this study discovered new types of platinum-containing selenide minerals: padmaite and sudovikovite [6, 7].

The third type is presented by mine-run and even base vanadium ores (vanadium concentration 0.3–3.0%) with a high content of secondary uranium–vanadium and uranium minerals. This type of ores is predominantly located at the field borders. These ores are characterized by the presence of carbonate and quartz–carbonate lodes with intense orange-yellow and reddish-orange (up to brown) secondary uranium mineralization. As seen from the XRD data, the ores contain typical minerals: calcite (45–50%), quartz (15%), carnotite $K_2(UO_2)_2V_2O_8 \cdot 3H_2O$ (15–30%), pentahydroborite $CaB_2O(OH)_6 \cdot 2H_2O$ (up to 10%), and sayrite $Pb_2(UO_2)_5O_6(OH)_2 \cdot 4H_2O$ (up to 15%). Based on the data of microprobe analysis, we revealed for the first time in ores of the Srednyaya Padma field microphases of such secondary minerals as kasolite $Pb(UO_2)SiO_4 \cdot H_2O$, vanuranylite $(H_3O, Ba, Ca)_{1.6} \cdot (UO_2)_2V_2O_8 \cdot 4H_2O$, vandendriesscheite $Pb(U^{6+})_7O_{22} \cdot 12H_2O$, and soddyite $(UO_2)_2SiO_4 \cdot 2H_2O$.

The prevailing components of the fourth type of ores are roscoelite micaites with small disseminations of selenides and secondary uranium mineralization. A sample of this type (P-804/21) was used in studies of water–rock interactions (see below).

Chemical State of Uranium in Minerals

Chemical shifts (δ) and relative line broadening (Γ) for four emission X-ray lines of the *L* series of uranium in the samples from Srednyaya Padma field, recorded with respect to $UO_{2.00}$ reference, are listed in Table 2. The positions of the samples in the coor-

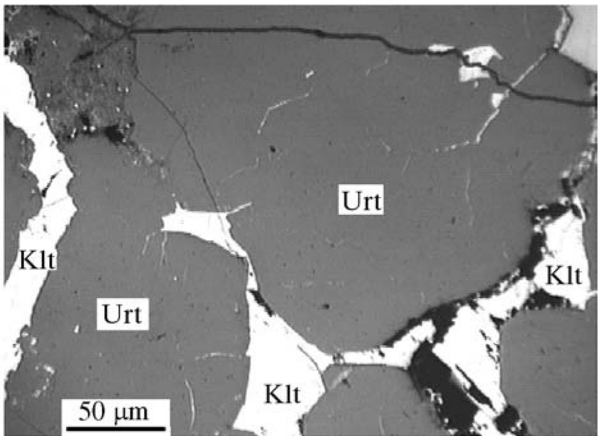

Fig. 1. Interrelation of uraninite (Urt) and clausthalite (Klt) in the lode uranium ore. Photomicrograph of the polished sections of PD-4 sample recorded in the incident light shows fine clausthalite veins in aggregate uraninite.

Table 3. Calculated contents of chemical and redox (IV, V, VI) forms of uranium and oxygen coefficients in uranium minerals of the Srednyaya Padma field

Sample	Uranium mineral	Weight fraction, % of total U minerals	Oxygen coefficient	Relative content, %			
				oxide form			uranyl form
				U(IV)	U(V)	U(VI)	
PD-3	Uraninite	100	2.26	59.2	29.3	11.5	0
PD-4	Uraninite	100	2.33	41.5	50.7	7.8	0
PD-5	Carnotite	85.7	3.00	0	0	0	85.7
	Uraninite	14.3	2.33	5.9	7.3	1.1	0
PD-6	Carnotite	50	3.00	0	0	0	50.0
	Sayrite	50	3.00	0	0	0	50.0

dinates of chemical shifts of the lines L_{α_1} and L_{β_1} are shown in Fig. 2. These experimental data show that there are two groups of uranium minerals strongly different in the chemical and redox state of uranium atoms. Samples PD-3 and PD-4 belonging to the second ore type contain predominantly U(IV) and U(V). Samples PD-5 and PD-6 (third ore type) occur near the right angle of the oxide diagram and contain U(VI) compounds [8]. Analysis of the content of various redox states of uranium using the algorithms given in [8] showed that least oxidized uraninite is typical for sample PD-3 in which the content of U(IV) is maximal and reaches 60%. Uraninite in sample PD-4 is more oxidized, but oxidation is limited only to the U(IV) → U(V) transformation. The content of U(VI) in both uraninites is similar and comprises 10±2% (Table 3).

The oxygen coefficients $(2 + x)$ in uranium oxides were calculated from the equation $x = 0.5p(\mathrm{V}) + 1.0p(\mathrm{VI})$, where $p(\mathrm{V})$ and $p(\mathrm{VI})$ are the fractions of uranium in minerals occurring in oxidation states (V) and (VI). Hence, the resulting oxygen coefficients of 2.26 and 2.33 in samples PD-3 and PD-4 correspond to U_4O_9 and U_3O_7. The oxygen coefficients for uranyl minerals were taken equal to 3.

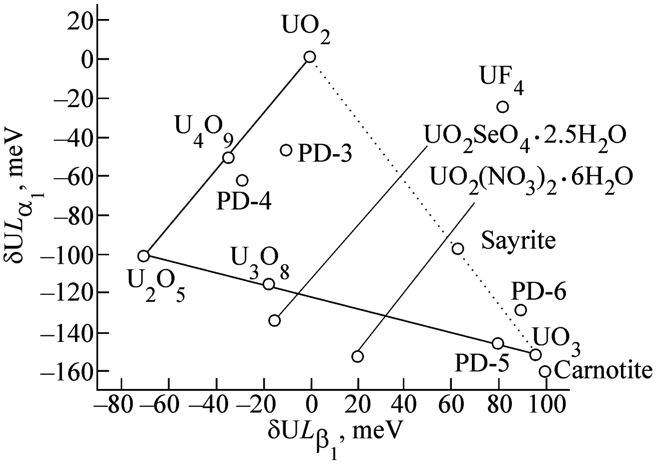

Fig. 2. Ore samples from the Srednyaya Padma field in the δUL_{α_1}–δUL_{β_1} coordinates (for comments, see text).

The parameters given in Table 2 for samples PD-5 and PD-6 characterize the composition of uranium mineral as a whole. Since δ and Γ are the additive quantities, we can calculate the corresponding parameters for individual uranium-containing components in these samples. An XRD analysis showed that, along with carnotite, sample DP-5 contains uraninite in the form of U_3O_7 (~5%), identical in the redox form to uraninite in sample PD-4. Hence, the experimental δ for sample PD-5 can be presented as a superposition of known shifts for sample PD-4 and unknown δ of carnotite. We can write four equations for four emission X-ray lines:

for L_{α_1}: $-146 = 0.857\delta + 0.143\times(-63)$,

for L_{α_2}: $+79 = 0.857\delta + 0.143\times(+21)$,

for L_{β_1}: $+81 = 0.857\delta + 0.143\times(-29)$,

for L_{γ_6}: $+541 = 0.857\delta + 0.143\times(+240)$,

and an equation to calculate the broadening of $L_{\gamma 6}$ lines

$$-1526 = 0.857\Gamma + 0.143\times(-821).$$

Solution of these equations gives required values for uranium in carnotite of sample PD-4 (Table 2). Thus, the coordinates of carnotite (δL_{α_1} and δL_{β_1}) are beyond the diagram (Fig. 2) and occur in the area typical for uranyl derivatives [9].

In accordance with XRD data, sample PD-6 contains equal amounts of two uranium mineral forms: carnotite and sayrite. Using the total values of δ and Γ of sample PD-6, we can calculate the partial quantities characterizing sayrite. Taking into account the above values of δ and Γ for carnotite, we can construct the following five equations:

for L_{α_1}: $-129 = 0.5\delta + 0.5 \times (-160)$,

for L_{α_2}: $+84 = 0.5\delta + 0.5 \times (+89)$,

for L_{β_1}: $+86 = 0.5\delta + 0.5 \times (+99)$,

for L_{γ_6}: $+497 = 0.5\delta + 0.5 \times (+591)$,

for $\Gamma(L_{\gamma_6})$: $-1534 = 0.5\Gamma + 0.5 \times (-1644)$.

The calculated values for sayrite and the corresponding point in the coordinates of chemical shifts of L_{α_1} and L_{β_1} are shown in Fig. 2. The position of sayrite at the boundary of the oxygen diagram can probably indicate that this mineral belongs to the oxide systems of UO_{2+x} type. To check this assumption, we studied the dependence of broadening of the L_{γ_6} line on the chemical shift δ of this line for several synthetic and natural uranium compounds. The results are shown in Fig. 3.

Previously we found that the broadening of the L_{γ_6} lines is determined by the interaction between the 5*f* and 6*d* electron functions of uranium atom [10]. In turn, this interaction is determined by the number of unpaired electrons on the 5*f* orbitals , i.e., by their spin density. The oxide systems with high accuracy follow a linear dependence describing the decrease of the spin density on 5*f* orbitals with increasing oxygen coefficient. Carnotite also does not deviate from this dependence, probably due to the diamagnetic properties of uranyl derivatives. Significant deviation is observed only in two cases: increased spin density for U(IV) halides and decreased spin density for sayrite [natural mineral $Pb_2(UO_2)_2(UO_4)_3(OH)_2 \cdot 4H_2O$]. Figure 3 suggests that the electronic structure of sayrite is strongly different from that of oxide and uranyl systems.

Interaction of Natural Waters with Vanadium Ores

We studied leaching of radionuclides of uranium series from ores of the Srednyaya Padma field at contact with various natural waters (in experiments, with model solutions simulating natural waters). In the experiments we used two samples of mineral compositions, which do not belong to vanadium ores strongly enriched with uranium. Sample no. 1 (P-804/21) was taken from hole no. 4836 from a depth of 113.7 m; it can be described as roscoelite micaite with small inclusions of gold–selenide and secondary uranium mineralization. The latter was presented by carnotite $K_2(UO_2)_2(VO_4)_2 \cdot 3H_2O$. The uranium content in this sample was 0.22 wt %, and the sample weight was 38 g. Sample no. 2 (P-733/61, hole no. 2822, depth 148.6 m) was the roscoelite breccia with the set of carbonate veins; it was taken from the set of samples characterizing mainly the second type of vanadium ores. The XRD data showed the presence of two uranium minerals, namely, carnotite and tyuyamunite $Ca(UO_2)_2(VO_4)_2 \cdot (5–8)H_2O$. The uranium content in this sample was 0.81 wt %, the sample weight was 13 g, and the radiation exposure dose was up to 100 μR h^{-1}. The total surface area of all the fractions of sample nos. 1 and 2 was 1.1 and 0.35 m^2, respectively. The data on the concentration of uranium and specific activity of ^{226}Ra and some products of its radioactive decay for both samples, determined by γ-ray spectrometry, are listed in Table 4.

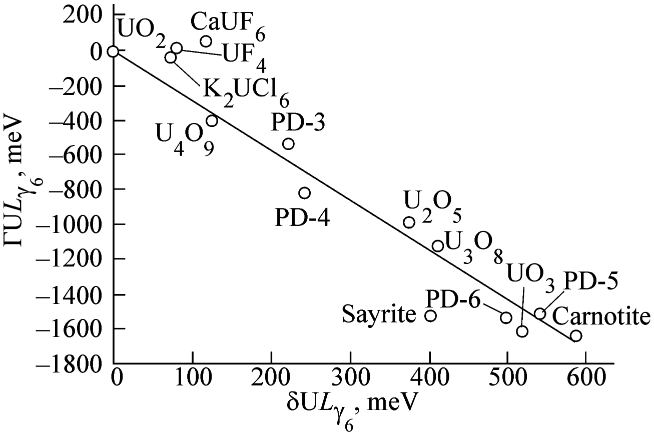

Fig. 3. Ore samples from the Srednyaya Padma field in the ΓUL_{γ_6}–δUL_{g_6} coordinates (for comments, see text).

As seen from Table 4, the fraction with the smallest grain size is the most enriched with radionuclides of the uranium series. This fact can be explained by both the small size of uranium minerals and their low strength due to which they pass into the finest fraction in the course of grinding. The given uranium contents correspond to ^{238}U activities in sample nos. 1 and 2 of 1035.5 and 1284.9 Bq.

Sample no. 1 was successively washed with 5 l of model atmospheric precipitates (aerated water) and then with mineralized water (1 l). Sample no. 2 was washed with aerated water (1 l) and with mineralized water (1 l). In each liter of the eluate, the α-activity of

Table 4. Concentration of uranium (mg g^{-1}) and specific activities of ^{226}Ra, ^{214}Pb, and ^{214}Bi (Bq g^{-1})

Fraction characteristics			Radionuclide			
number*	weight, g	size, mm	^{238}U	^{226}Ra	^{214}Pb	^{214}Bi
1-1	10.181	0.25–0.50	2.29	27.7	24.2	24.8
1-2	10.649	0.12–0.25	2.24	27.2	22.8	23.8
1-3	14.742	0.07–0.12	2.08	25.1	21.8	23.3
1-4	2.933	0.01–0.07	2.64	32.0	27.3	28.1
2-1	4.989	0.25–0.50	7.27	88.0	87.4	84.5
2-2	2.981	0.12–0.25	8.55	103.5	99.6	103.4
2-3	4.018	0.07–0.12	7.55	91.5	84.5	82.3
2-4	1.176	0.01–0.07	11.9	144.3	125.6	124.0

* The first and second figures are the numbers of sample and eluate, respectively; the same for Tables 5–8.

Table 5. Activity of uranium isotopes in eluates from sample nos. 1 and 2

Fraction number	^{238}U, counts h^{-1}	^{234}U, counts h^{-1}	^{238}U, Bq l^{-1}	^{234}U/^{238}U, Bq/Bq	^{238}U, Bq l^{-1} m^{-2} day^{-1}	Leached ^{238}U, %
1-1	–	–	–	2.11 ± 0.06	–	0.26
1-4	1738	2500	1.58	1.44 ± 0.08	0.96	0.13
1-5	1670	1880	1.52	1.13 ± 0.06	0.92	0.13
1-6	5470	5980	4.96	1.10 ± 0.04	1.5	0.21
2-1	9450	9800	8.57	1.04 ± 0.02	25	2.1
2-2	21770	22490	19.73	1.03 ± 0.02	56	4.9

^{228}U and ^{234}U was determined. The leaching results are listed in Table 5.

Our experimental results show that natural waters can be strongly polluted with uranium isotopes, though the normalized activities of eluates obtained from sample no. 1 do not exceed the maximum permissible concentration of radionuclides in drinking water, comprising 2.9 and 3.1 Bq l^{-1} for ^{234}U and ^{238}U, respectively [11]. The maximum permissible concentration was somewhat exceeded only for sample no. 2 under the effect of both model atmospheric precipitates and especially model ground waters.

As seen from the data on γ-activity of Ba(Ra, Pb) · SO_4 preparations, the leaching of ^{226}Ra from roscoelite with the uranium concentration of 0.22% is insignificant. In most cases the radioactivity of ^{226}Ra and its daughter nuclides ^{214}Pb and ^{214}Bi is below the detection limit of ~0.6 Bq. When the content of uranium was 0.81% (sample no. 2), leaching of ^{226}Ra was readily recorded. The data on the activity of its daughter nuclides (Table 6) showed that the normalized content of radium in the model atmospheric precipitates and ground water was 14 and ~22 Bq l^{-1} m^{-2} day^{-1}, respectively. Comparison of these data with those given in Table 5 shows that the rate of uranium leaching is higher than that of radium, especially in the case of mineralized waters, when the leaching rate of uranium reaches 56 Bq l^{-1} m^{-2} day^{-1}. This effect is probably due to the significant concentration of carbonate and sulfate ions in the mineralized water. Taking into account that the maximal permissible concentration of ^{226}Ra is 0.5 Bq l^{-1}, the normalized concentrations of uranium and radium in the resulting eluates exceed the permissible values by a factor of 20–40 [11]. ^{234}U passes from the ore into the solution simulating atmospheric precipitates to a greater extent than does ^{238}U. The ^{234}U/^{238}U activity ratio for some eluates reaches 2.1, which suggests

Table 6. γ-Ray activity of ^{214}Pb and ^{214}Bi and calculated normalized activity of ^{226}Ra in eluates from sample nos. 1 and 2

Fraction number	Leaching time, days	^{214}Pb, Bq l^{-1}	^{214}Bi, Bq l^{-1}	^{226}Ra, Bq l^{-1} m^{-2} day^{-1}
1-6	3	2.1 ± 1	1 ± 1	0.3–0.6
2-1	1	4.8 ± 1	5.3 ± 1	13.7–15.1
2-2	1	8.1 ± 1	7.8 ± 1	22.3–23.1

Table 7. β-Ray activity normalized to 1 l of model solutions

Fraction number	N_{av}, counts	$N_{av} - N_{backgr}$, counts	Error, counts	Activity, Bq l^{-1}	Leaching time, days
1-1	258	31	10	13 ± 5	2
1-2	283	56	10	4 ± 1	1.5
1-3	337	110	11	6 ± 1	1.5
1-4	444	217	12	8 ± 2	1.5
1-5	264	37	10	7 ± 2	1.5
1-6	674	447	14	27 ± 5	3
2-1	1277	1050	17	75 ± 14	1
2-2	1073	846	17	103 ± 21	1
Background	227		7		
Reference	1467	1240	20	15 ± 3	

significant contribution of nuclear-chemical effects to leaching of radiogenic nuclides.

The leaching effect is the most pronounced in the series $^{210}Pb \rightarrow {}^{210}Bi \rightarrow {}^{210}Po$. This conclusion can be made from the data on β-ray activity of $BaSO_4$ precipitates, which can belong to four emitters of the ^{226}Ra series: ^{214}Pb, ^{214}Bi, ^{210}Pb, and ^{210}Bi. Since the contribution of the first two nuclides was determined previously by γ-ray spectrometry, we can evaluate the β-ray activity of ^{210}Pb and ^{210}Bi radionuclides. The data on the β-ray activity of $BaSO_4$ preparations (average of four 1000-s measurements) are listed in Table 7; the activities were normalized with respect to the specific surface area (1 m^2) and leaching time (1 day). The resulting data are listed in Table 8. The activities of $^{210}Pb(^{210}Bi)$ were calculated using the data from Table 6.

Thus, at 0.81% content of uranium in roscoelite breccia, the normalized activity of leaching solutions with respect to ^{210}Pb reaches 185–248 Bq l^{-1} m^{-2} day^{-1}. As seen from [11], this value exceeds the maximum permissible level (0.2 Bq l^{-1}) by at least three orders of magnitude. To confirm that exactly the β-ray activity of compounds of the ^{210}Pb series is recorded in the sources, $BaSO_4$ precipitates were treated with HCl, the solutions were evaporated, and the α-activity of the residues was measured. The resulting spectra showed the presence of an α-emitter with the upper energy level of 5.3 MeV, i.e., ^{210}Po. Since ^{210}Po occurs in the secular equilibrium with ^{210}Pb, its activity is equal to the activity of mother isotope Pb, and the maximal permissible concentration is even lower (0.12 Bq l^{-1}) [11]. These results suggest that violation of environmental requirements in the course of mining of uranium-vanadium ores of the Srednyaya Padma field can cause pollution of the aquatic ecosystem of the northern regions near Lake Onega with β-emitters of uranium series.

Table 8. Normalized β-activity of the model solutions, Bq l^{-1} m^{-2} day^{-1}

Fraction no.	Total β-activity	$^{210}Pb(^{210}Bi)$ activity
1-1	6	6
1-2	4	4
1-3	4	4
1-4	5	5
1-5	4	4
1-6	8	6
2-1	214	185
2-2	294	248

ACKNOWLEDGMENTS

This study was financially supported by the Russian Foundation for Basic Research (project no. 02-05-97513).

REFERENCES

1. Sumbaev, O.I., *Kristall-difraktsionnye gamma-spektrometry* (Crystal Diffraction γ-Ray Spectrometers), Moscow: Gosatomizdat, 1963.
2. Andreev, S.E., Tovarov, V.V., and Perov, V.A., *Zakonomernosti izmel'cheniya i ischisleniya kharakteristik granulometricheskogo sostava* (Principles of Grinding and Evaluation of Grain-Size Characteristics), Moscow: Metallurgizdat, 1959.
3. *Radiometricheskie metody analiza estestvennykh elementov* (Methods of Radiometric Analysis of Natural Elements), Zheleznova, E.I., Shumilin, I.P., and Yufa, B.Ya., Eds., Moscow: Nedra, 1968.
4. *Khimiya urana: Sbornik nauchnykh trudov* (Uranium

Chemistry: Coll. of Scientific Papers), Laskorin, B.N. and Myasoedov, B.F., Eds., Moscow: Nauka, 1989, pp. 171–178.

5. Bogdanov, R.V., Kozak, P.P., and Tupitsyn, I.I., *Vestn. Sankt-Peterb. Gos. Univ., Ser. 4*, 1995, no. 4, pp. 65–71.
6. Polekhovskii, Yu.S., Voloshin, A.V., Tarasova, I.P., et al., *Zap. Vses. Mineral. O-va.*, 1991, no. 3, pp. 85–88.
7. Polekhovskii, Yu.S., Tarasova, I.P., Nesterov, A.R., et al., *Dokl. Ross. Akad. Nauk*, 1997, vol. 354, no. 1, pp. 82–85.
8. Bogdanov, R.V., Batrakov, Yu.F., Puchkova, E.V., and Sergeev, A.S., *Radiokhimiya*, 1999, vol. 41, no. 5, pp. 385–408.
9. Batrakov, Yu.F., Bogdanov, R.V., Puchkova, E.V., and Sergeev, A.S., *Radiokhimiya*, 2000, vol. 42, no. 2, pp. 106–112.
10. Krivitsky, A.G., Bogdanov, R.V., and Batrakov, Yu.F., Extended Abstracts, *6th Int. Conf. on Nuclear and Radiochemistry*, Aachen, 2004, vol. 3, pp. 92–94.
11. *Normy radiatsionnoy bezopasnosti: gigienicheskie normativy (NRB-99)* (Standards of Radiation Safety: Hygienic Regulations (NRB-99)), Moscow: Minzdrav, 1999.